INVESTIGATION ON THE THREE-DIMENSIONAL MULTIPHASE CONJUGATE CONDUCTION PROBLEM INSIDE POROUS MEDIA WITH THE LATTICE BOLTZMANN METHOD

Kai Zhao, Li Qiang, Yimin Xuan
School of Power Engineering
Nanjing University of Science & Technology
Nanjing 210094, China
Tel/Fax: 02584315488; E-mail: liqiang@mail.njust.edu.cn

Abstract

A new mesoscopic approach has been developed for investigating the heat conduction process inside the three-dimensional random porous media. Then heat transfer model is established at the pore scale of the random porous layer. The multiphase conjugate energy transport equations are solved by means of the lattice Boltzmann method. Then this new approach has been used to investigate the transient heat conduction process inside the porous wick of CPLs/LHPs at pore scale, which is vital for analyzing the startup stability of a CPLs/LHPs. The results show that this new numerical algorithm is rigorous, general and robust for simulating the heat conduction process in the complex structure.

KEYWORDS

Heat conduction, pore scale, porous media, lattice Boltzmann method.

INTRODUCTION

Transport phenomena in porous media have been investigated for many years for applications in materials, agricultural, and petroleum engineering. Recently, more interests have been focused on heat and mass transfer processes in microporous media due mainly to their increasing importance in thermal engineering, such as Capillary Pumped Loops (CPLs), and Loop Heat Pipes (LHPs) [1, 2].

As is well-known, the evaporator with the capillary porous structure is the primary functional component which accepts heat fluxes, organizes evaporation and produces driving force of the working fluid flowing circularly in the whole CPLs/LHPs. Heat transfer with flow and evaporation occurs just in the microporous media. For the security and efficiency of CPLs/LHPs performance, it is important and necessary to investigate the dynamic and thermodynamic behavior of the working fluid in microporous media. Although there have been many studies in this field [3–6], two shortcomings exist in current researches. Firstly, current researches to CPLs/LHPs focus on transient characters and the previous works in literatures stayed at the simulation or experiments of steady heat transfer in the capillary wick. Steady mathematical models cannot simulate the development of flow field in porous media from start-up to a steady working state or the response of flow field on the transition between different steady working state [7, 8]. Secondly, the literatures only focus on the N-S equation with the continuous assumption, not considering the microstructures of the porous media which is very important to energy transport in the mircoporous media. The objective of this work is to develop a comprehensive approach for more accurate prediction of the transient heat conduction processes in microporous media at pore scale. To achieve this, we will first adopt a lattice Boltzmann method to describe the three-dimensional multiphase conjugate heat conduction problem by means of a spatially varying relaxation time. With the LB method, one can conveniently consider the structural characteristics of the wick layer and ensures the continuous constraints along the interfaces among the solid matrices and the fluid. Next we use the statistical method to reconstruct the three-dimensional random microporous media. The present method has been applied to simulate the heat conduction processes in the evaporator with microporous structure of the CPLs/LHPs at pore scale.

1. NUMERICAL METHODS

1.1. Governing equations

The energy equations for pure heat conduction processes in the two phase system, e.g. fluid and solid, without heat sources are

$$(\rho c_p)_f(\frac{\partial T}{\partial t}) = k_f \nabla^2 T \ , \tag{1}$$

$$(\rho c_p)_s(\frac{\partial T}{\partial t}) = k_s \nabla^2 T \ , \tag{2}$$

where subscript f represents the fluid, and s the solid; T is the temperature, ρ the density, k the thermal conductivity, and c_p the specific heat capacity.

At the interface between the two phases, the temperature and heat flux have to be satisfied with no contact thermal resistance at the interfaces.

$$T_{f,\text{int}} = T_{s,\text{int}} \ , \tag{3}$$

$$k_f \left.\frac{\partial T}{\partial n}\right|_{f,\text{int}} = k_s \left.\frac{\partial T}{\partial n}\right|_{s,\text{int}} \ , \tag{4}$$

where the subscript "int" corresponds to the interfaces and n represents the unit normal vector to the interfaces. Eqs. (1)–(4) can be numerically solved by the finite deference or finite volume methods in classical CFD codes. However, when the geometries are too complex, the CFD may meet unacceptable. So a new efficient approach must be proposed.

1.2. Lattice Boltzmann model

The lattice Boltzmann method (LBM) is intrinsically a mesoscopic approach based on the evolution of statistical distribution of lattices and has achieved considerable success in simulating fluid flows and associated transport phenomena [9–11]. It was proved the lattice BGK method was consistent with the Navier-Stokes equation for fluid flow through Chapman-Enskog expansion. The most important advantages of LBM are the easy implementation of multiple interparticle interactions and complex geometry boundary conditions [12,13]. Nowadays, the lattice evolution methods have been used to solve most of the thermal behaviors [14, 15]. Here a new three-dimensional lattice Boltzmann model is developed for the fluid-solid conjugate pure heat conduction problem. Eqs. (1), (2) are pure diffusive equations, have not convection term. It is well known that 90° rotational invariance is sufficient to yield full isotropy for pure diffusive phenomena and a square or a cubic lattice in two or three dimensions is enough, respectively [16]. Here the three-dimensional seven-speed (D3Q7), shown in Fig. 1 lattice model has been proposed to describe the eqs. (1), (2).

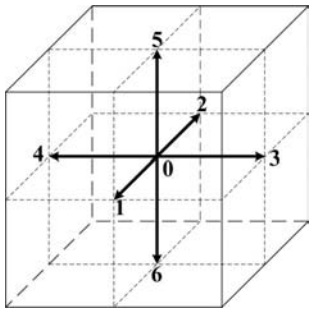

Fig. 1. The lattice of D3Q7

The evolution equation for D3Q7 LBM in both solid and liquid phases can be generally given as [17]

$$T_\alpha(\mathbf{r}+\mathbf{e}_\alpha\delta_t, t+\delta_t) - T_\alpha(\mathbf{r},t) = -\frac{1}{\tau}[T_\alpha(\mathbf{r},t) - T_\alpha^{eq}(\mathbf{r},t)] \ , \tag{5}$$

where $\mathbf{r}$ is the location vector, t is the real time, δ_t the time step, $\alpha = 0,1,...6$ the direction of the discrete lattice speed. T_α^{eq} the equilibrium distribution function

$$T_\alpha^{eq} = \frac{1}{7}T \ , \tag{6}$$

$\mathbf{e}_\alpha$ is the discrete velocity. For the D3Q7 model it is given as

$$\mathbf{e}_\alpha = \begin{bmatrix} 0 & c & -c & 0 & 0 & 0 & 0 \\ 0 & 0 & 0 & c & -c & 0 & 0 \\ 0 & 0 & 0 & 0 & 0 & c & -c \end{bmatrix} \tag{7}$$

and τ the dimensionless relaxation time for each phase, c is a lattice speed, also a pseudo sound speed, defined as δ_x / δ_t, where δ_x is the grid size.

Eqs. (1), (2) can be obtained from eq. (5) through Chapman-Enskog expansion, also the macroscopical thermal diffusivity of each phase which is determined by the corresponding τ is

$$D_s = \frac{2}{7} c^2 (\tau_s - 0.5)\delta_t \tag{8}$$

and

$$D_f = \frac{2}{7} c^2 (\tau_f - 0.5)\delta_t \ , \tag{9}$$

where D_s and D_f are the thermal diffusivity of the solid phase and the fluid phase respectively, defined as $k_s/(\rho c_p)_s$, $k_f/(\rho c_p)_f$. Especially, for liquid flow, c can take any positive value theoretically only to insure τ to be within (0.5, 2) [18, 19]. A larger c may result in a more accurate temperature prediction near the boundaries, yet with higher computational costs. The temperature and the heat flux can then be calculated as

$$T = \sum_\alpha T_\alpha \ , \tag{10}$$

$$\mathbf{q} = (\sum_\alpha \mathbf{e}_\alpha T_\alpha) \frac{\tau - 0.5}{\tau} \rho c_p \ , \tag{11}$$

where ρc_p is the volume thermal capacity of each phase.

1.3. Deduction of eq. (11)

The evolution equation for the temperature field without heat source proposed by He *et al.* is [15]

$$\bar{g}_\alpha(\mathbf{r} + \mathbf{e}_\alpha \delta_t, t + \delta_t) - \bar{g}(\mathbf{r}, t) = -\frac{\delta_t}{\tau_g + 0.5\delta_t}[\bar{g}(\mathbf{r}, t) - g^{eq}(\mathbf{r}, t)] \tag{12}$$

and

$$\rho e = \sum_\alpha \bar{g}_\alpha - \frac{\delta_t}{2} \sum_\alpha f_\alpha Z_\alpha \ , \tag{13}$$

$$\mathbf{q} = (\sum_\alpha \mathbf{e}_\alpha \bar{g}_\alpha - \rho e \mathbf{u} - \frac{\delta_t}{2} \sum_\alpha \mathbf{e}_\alpha f_\alpha Z_\alpha) \frac{\tau_g}{\tau_g + 0.5\delta_t} \ , \tag{14}$$

where the Z_α represents the effects of viscous heating and $\mathbf{u}$ is the speed of the flow, e the thermal energy density. Here, the effects of viscous heating is ignored and for the pure heat conduction problem, $\mathbf{u} = 0$. So eqs. (13), (14) can be predigested as

$$\rho e = \sum_{\alpha} \overline{g}_{\alpha} \ , \tag{15}$$

$$\mathbf{q} = (\sum_{\alpha} \mathbf{e}_{\alpha} \overline{g}_{\alpha}) \frac{\tau_g}{\tau_g + 0.5\delta_t} \ . \tag{16}$$

As is well-known, the thermal energy density for general liquid is expressed as follows:

$$e = c_p T \ . \tag{17}$$

Compare eqs. (5)–(10) with eqs. (12)–(15) and reminding eq. (17), we can write

$$\tau = \frac{\tau_g}{\delta_t} + 0.5 \ , \tag{18}$$

$$T_{\alpha} = \frac{\overline{g_{\alpha}}}{\rho c_p} \ . \tag{19}$$

Substituting eqs. (19)–(18) into eq. (16), the expression of the heat flux (i.e. eq. (11)) in our model can be obtained.

1.4. Boundary conditions

Boundary conditions play important roles in lattice Boltzmann methods in that they will influence the accuracy and stability of the LBM. Considering there are too many boundaries for the three-dimensional problem, for the thermal boundaries conditions, we follow the nonequilibrium extrapolation rule proposed by Guo which is of second order and has better numerical stability [20].

$$T_{\alpha}(\mathbf{x}_b, t) = T_{\alpha}^{eq}(\mathbf{x}_b, t) + T_{\alpha}^{neq}(\mathbf{x}_f, t) \ , \tag{20}$$

where the subscripts b and f represent the node on the boundary and the nearest neighbour fluid node of $\mathbf{x}_b$, respectively. The nonequilibrium term $T_{\alpha}^{neq}(\mathbf{x}_f, t)$ represents the deviation from the equilibrium, which is defined as:

$$T_{\alpha}^{neq}(\mathbf{x}_f, t) = T_{\alpha}(\mathbf{x}_f, t) - T_{\alpha}^{eq}(\mathbf{x}_f, t) \ . \tag{21}$$

So for the isothermal boundary treatment, the temperature distribution is given by

$$T_{\alpha}(\mathbf{x}_b, t) = T_{\alpha}^{eq}(\mathbf{x}_b, t) + T_{\alpha}(\mathbf{x}_f, t) - T_{\alpha}^{eq}(\mathbf{x}_f, t). \tag{22}$$

Alternately, for the heat flux boundary treatment, $T_{\alpha}(\mathbf{x}_b, t)$ is given by

$$T_{\alpha}(\mathbf{x}_b, t) = \overline{T_{\alpha}^{eq}}(\mathbf{x}_b, t) + T_{\alpha}(\mathbf{x}_f, t) - T_{\alpha}^{eq}(\mathbf{x}_f, t) \ , \tag{23}$$

where $\overline{T_{\alpha}^{eq}}(\mathbf{x}_b, t)$ is an approximation to $T_{\alpha}^{eq}(\mathbf{x}_b, t)$ defined by

$$\overline{T_{\alpha}^{eq}}(\mathbf{x}_b, t) = \frac{T(\mathbf{x}_f, t) + (q \cdot \delta_x)/k}{7} \ , \tag{24}$$

where q is the heat flux on the boundary and k is the conductivity of the liquid.

These boundary treatments above are very suitable for the complex three-dimensional geometry and also have a second order accuracy.

2. RESULTS AND DISCUSSION

2.1. Heat conduction process in the evaporator of CPLs at pore scale

In the following simulations, we focus on a cubic system each side of which is 6.4 μm long. A $64 \times 64 \times 64$ uniform gird is used. Such a cell is schematically shown in Fig. 2. The process for the three-dimensonal random porous media can refer [21]. The average pore and particle diameters of our capillary wick are around 1 and 2.6 μm, that means each particle or pore has about 10 nodes averagely, which is necessarily for the simulation in the poroous media. But such a small diameter restricts the size of the computational domain. The larger domain drives the computational cost up often to an unrealistic level due to the three-dimensional nature of this study. In Fig. 2, the boundary conditions are described below.

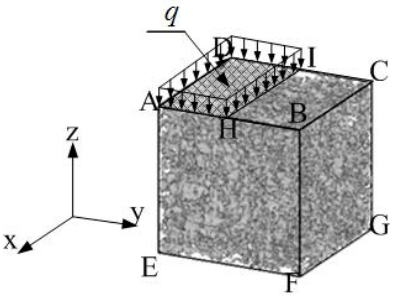

Fig. 2. Schematic of the computational cell

At surface EAD and BFGC

$$\frac{\partial T}{\partial y} = 0 \ , \tag{25}$$

at surface AEFB and DCG

$$\frac{\partial T}{\partial x} = 0 \ , \tag{26}$$

at surface AHID

$$-k \frac{\partial T}{\partial z} = q \ , \tag{27}$$

at surface EFG

$$T = T_{in} \ , \tag{28}$$

at surface HBCI

$$\frac{\partial T}{\partial z} = 0 \ . \tag{29}$$

Table 1. Some properties for the evaporator

	Matrix part	Working fluid
Material	Nickel	Ammonia
Conductivity (W/(m·K))	91	0.525
Density (kg/m^3)	8900	620
Specific heat capacity (J/kg· K)	460	4600
Saturated temperature (K)	275	
Entrance temperature (K)	265	

Table 1 gives the physical properties used in the present simulation.

2.1.1 Results

Fig. 3 shows the temperature distributions at different time in the three-dimensional space. The isotherms are not smooth and different at different positions due to the random microstructures of the porous media and this phenomenon cannot be simulated using the conventional CFD methods easily, unless doing the simulation at the pore scale, just like the present D3Q7 model. Compare Fig. 3 (a) and (b), we find that when the evaporator start-up, the isotherms near the fin where the heat flux is loaded are quite flexuous and after starting-up, the energy transfer downwards along the z axis, the isotherms move downwards and go to the steady-state. Although, we only consider pure heat conduction process here, according to the flexuous isotherms, we can judge that the phase interface during the phase change process is not smooth as well due to the random structure of the porous media and this phenomenon cannot be discovered by the conventional CFD.

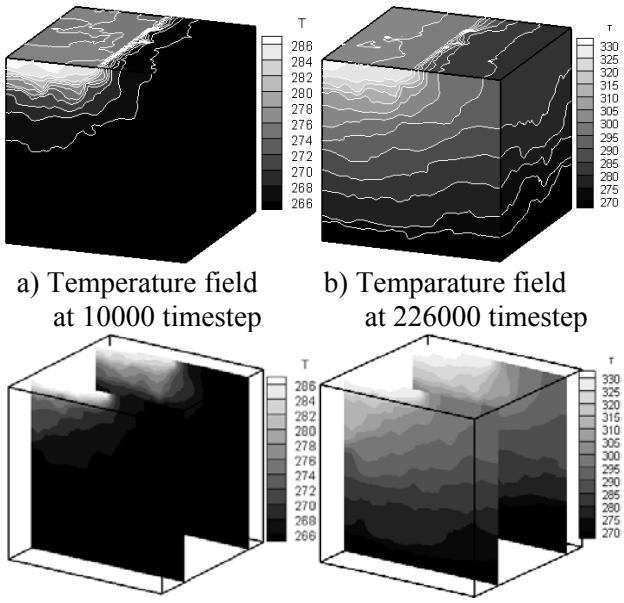

a) Temperature field at 10000 timestep b) Temparature field at 226000 timestep

c) Slice of the field at 10000timestep d) Slice of the field at 226000 timestep

Fig. 3. Temperature distribution for $q = 1.0 \times 10^8$ W/m^2

Fig. 4 shows the calculated average temperature versus the time. The time changes from 0 to 226000 steps. The results show that the average temperature increases with the time. The increasing rate rises with the time as well which is very sharp when the time is smaller than 50000 steps and becomes very low when the time is larger than 150000 steps. Obviously, it is not a linear relation.

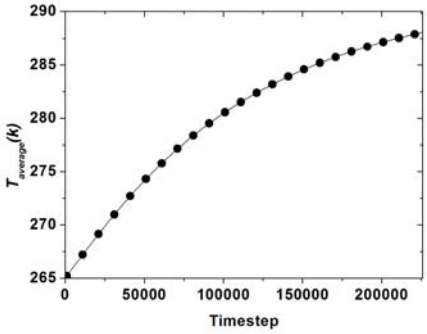

Fig. 4. The average temperature versus timestep

2.1.2 Heat flux effects

Fig. 5 shows the the influence of the heat flux to the time when the first fluid node reaches the saturated temperature. The heat flux changes from 5×10^7 to 9×10^8 W/m^2. Other parameters are the same with Table 3. The results show that the time decreases quickly with the heat flux. According to the LB simulation results (see the hollow circle in Fig. 5), we guess that it satisfies the second-order exponential decay function, the reference line in Fig. 5 is the result by non-linear fit. Amazedly, they agree with each other very well. It indicates that the timestep versus the heat flux as a second-order exponential decay function in the evaporator of our CPLs. The function has been caculated as follows

$$timestep = 133.91272 + 28456.77264\exp(-q/3.0337\times10^7) + 2447.95304\exp(-q/1.53349\times10^8).$$

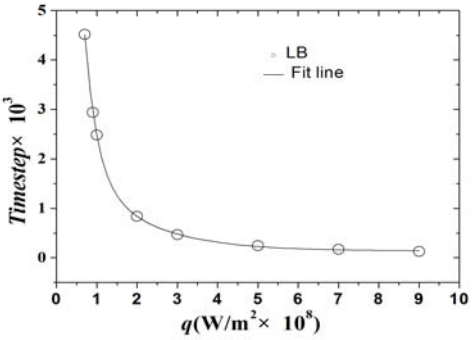

Fig. 5. The timestep when the first fluid node reaches the satruated temperature at different heat flux

Using this function, the time when the first fluid node reaches the saturated temperature (i.e. the time when the phase change first occurs) can be predicted at any heat flux.

3. CONCLUSIONS

Heat conduction process in the evaporator of CPLs has been numerically investigated using the mesoscopic simulation methods. Statistical method has been developed for reconstructing three-dimensional random microporous media and a lattice Boltzmann algorithm (D3Q7) considering multi-phase conjugate heat transfer was then developed to tackle the thermal conduction phenomena in the multiphase three-dimensional porous media with second-order accurate boundary treatments. Such a full numerical set is quite suitable for analyses of energy and mass transport in microporous media. The present model has then been applied to investigate the heat conduction process in the evaporator of CPLs/LHPs at pore scale which is very important to the start-up of the whole CPLs/LHPs.

The numerical modeling of the heat conduction process in the evaporator indicates that the random structure of the wick makes the temperature field not so smooth and the isotherms very flexuous, so we can predict that when phase change occurs in the evaporator, the liquid-vapor interface is not smooth at all due to the random structure which cannot be predicted based on the macroscopic theory and this indicates that the microstructures of the porous media has been correctly taken into account in our present model and it can predict the energy transport process in the complex structure more accurately. The results and methodology in this contribution may be of great significance for improving our understandings of heat transport mechanisms in two-phase microporous media, such as CPLs/LHPs.

Acknowledgments

This work is sponsored by the National Science Foundation of China (No. 50576038) and the Youth Scholar Foundation of Nanjing University of Science & Technology (No. Njust200402).

References

1. Theodore D., Swanson. NASA thermal control technologies for robotic // *Spacecraft Applied Thermal Engineering*, 2003, Vol. 23, pp. 1055–1065.
2. Yu F., Maydanik. Review Loop heat pipes // *Applied Thermal Engineering,* 2005, Vol. 25, pp. 635-657.
3. Cao Y., Faghri A. Analytical Solutions of Flow and Heat Transferin a Porous Structure with Partial Heating and Evaporation on the Upper Surface // *Intern. J. of Heat and Mass Transfer,* 1994, Vol. 36 (suppl. 10), pp. 1525-1533.

4. Cao Y., Faghri A. Conjugate Analysis of a Flat-Plate Type Evaporator for Capillary Pumped Loop with Three-Dimensional Vapor Flow in the Groove // *Intern. J. of Heat and Mass Transfer,* 1994, Vol. 37 (suppl. 3), pp. 401-409
5. Tarik Kaya, John Goldak. Numerical analysis of heat and mass transfer in the capillary structure of a loop heat pipe // *Intern. J. of Heat and Mass Transfer,* 2006, Vol. 49, pp. 3211-3220.
6. Chuan R., Qing-Song W., Mao-Bin H. Heat transfer with flow and evaporation in loop heat pipe's wick at low or moderate heat fluxes // *Intern. J. of Heat and Mass Transfer,* 2007, Vol. 50, pp. 2296-2308.
7. Khrustalev D., Faghri A. Heat transfer in the inverted meniscus type evaporator at high heat fluxes // *Intern. J. of Heat and Mass Transfer,* 1995, Vol. 38 (suppl. 16), pp. 3091-3101.
8. Zhao T.S., Liao Q. On capillary-driven flow and phase-change heat transfer in a porous structure heated by a finned surface: measurements and modeling // *Intern. J. of Heat and Mass Transfer,* 2000, Vol. 43, pp. 1141-1155.
9. Benzi R., Succi S., Vergassola M. The lattice-Boltzmann equation: theory and applications // *Phys. Report,* 1992, Vol. 222, pp. 145-197.
10. Qian Y., Succi S., Orszag S. Resent advances in lattice Boltzmann computing // *Annu. Rev. Comp. Phys*, 1995, Vol. 3, pp. 195-242.
11. Chen S., Doolen G. Lattice Boltzmann method for fluid flows // *Annu. Rev. Fluid Mech,* 1998, Vol. 1998, Vol. 30, pp. 329-364.
12. Pan C., Hilpert M., Miller C.T. Lattice-Boltzmann simulation of two-phase flow in porous media // *Water Resources Research,* 2004, Vol. 40, pp. 1-14.
13. Pan C., Prins J. F., Miller C. T. A high-performance lattice Boltzmann implementation to model flow in porous media // *Computer Physics Communications,* 2004, Vol. 158, pp. 89-105.
14. Orazio A. D., Succi S., Arrighetti C. Lattice Boltzmann simulation of open flows with heat transfer // *Physics of fluids,* 2003, Vol. 15, pp. 2778-2781.
15. He X., Chen S., Doolen G. A novel thermal model for the lattice Boltzmann method in incompressible limit // *J. of computational physics,* 1998, Vol. 146, pp. 282-300.
16. Toffoli T., Margolus N. Invertible cellular automata: A review // *Physica D,* 1990, Vol. 45, pp. 229-253.
17. Guo Z. L., Zheng C. G., Li Q., Wang N. C. Lattice Boltzmann Method For Hydrodynamics, Technology Press, Hubei, 2002, pp. 111-125 (China).
18. Kang Q. J., Zhang D. X., Lichtner P. C., Tsimpanogiannis I. N. Lattice Boltzmann model for crystal growth from supersaturated solution // *Geophys. Res. Lett,* 2004, Vol. 31, pp. L21604.
19. Wang J., Wang M., Li Z. A lattice Boltzmann algorithm for fluid-solid conjugate heat transfer // *Intern. J. of Thermal Sciences,* 2007, Vol. 46, pp. 228-234.
20. Guo Z. L., Shi B. C., Zheng C. G. A coupled lattice BGK model for Boussinesq equations // *Intern. J. for Numerical Methods in Fluids,* 2002, Vol. 39, pp. 325-342.
21. Zhao K., Li Q., Xuan Y. M. A reconstruction technique for three dimensional porous media from 2D image // *The 2007 Asian Symposium "Computational Heat Transfer and Fluid Flow", Xi'an, China,* 2007.